Supplementary Information

Two-step synthesis of luminescent MoS$_2$-ZnS hybrid quantum dots

Rhiannon M. Clark,[a,b] Benjamin J. Carey,[a,b] Torben Daeneke,*[a] Paul Atkin,[a,b]

Madhu Bhaskaran,[c] Kay Latham,[d] Ivan S. Cole[b] and Kourosh Kalantar-zadeh*[a]

[a.]   School of Electrical and Computer Engineering, RMIT University, Melbourne, Victoria, 3001, Australia
[b.]   Manufacturing Flagship, CSIRO, Clayton, Victoria, 3169, Australia
[c.]   Functional Materials and Microsystems Research Group, RMIT University, Melbourne, Victoria, 3000, Australia
[d.]   School of Applied Science, RMIT University, Melbourne, Victoria, 3001, Australia

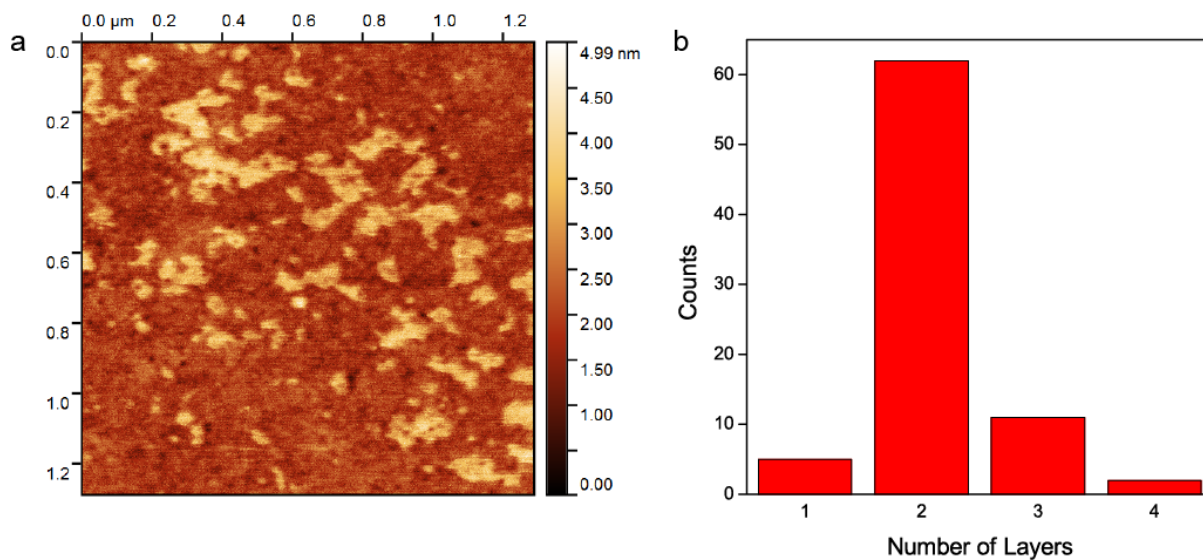* Torben.daeneke@rmit.edu.au, Kourosh.kalantar@rmit.edu.au

Figure S1. AFM characterisation of exfoliated MoS_2. (a) AFM image. (b) Flake height histogram of 80 flakes in (a).
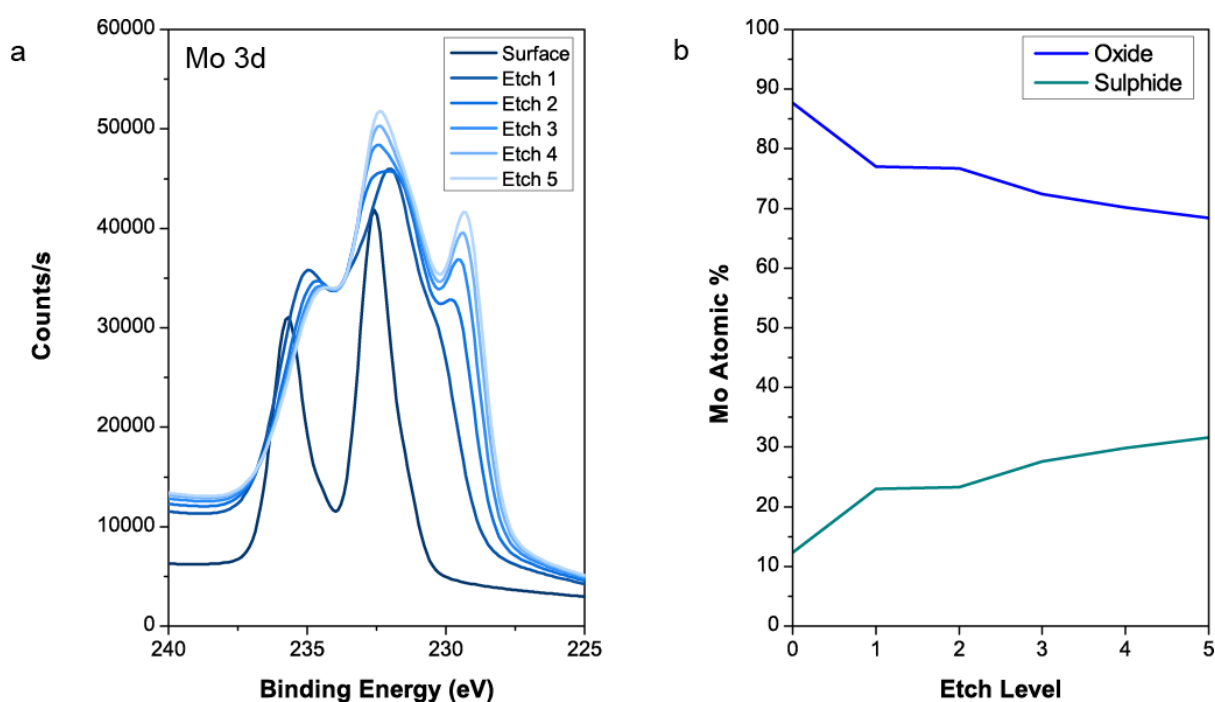

Figure S2. XPS etch level analysis of exfoliated MoS_2: (a) Mo 3d energy range at different etch levels showing Mo^{6+} at the surface and the evolution of the peaks for Mo^{4+}. (b) Atomic percentage profile of Mo^{6+} (oxide) and Mo^{4+} (sulphide).
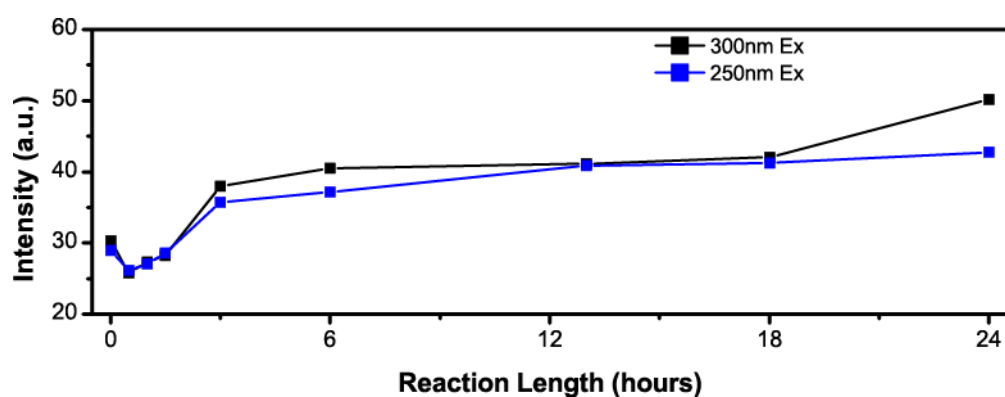
Figure S3. PL emission from MoS$_2$ QDs hydrothermally processed for different lengths of time.
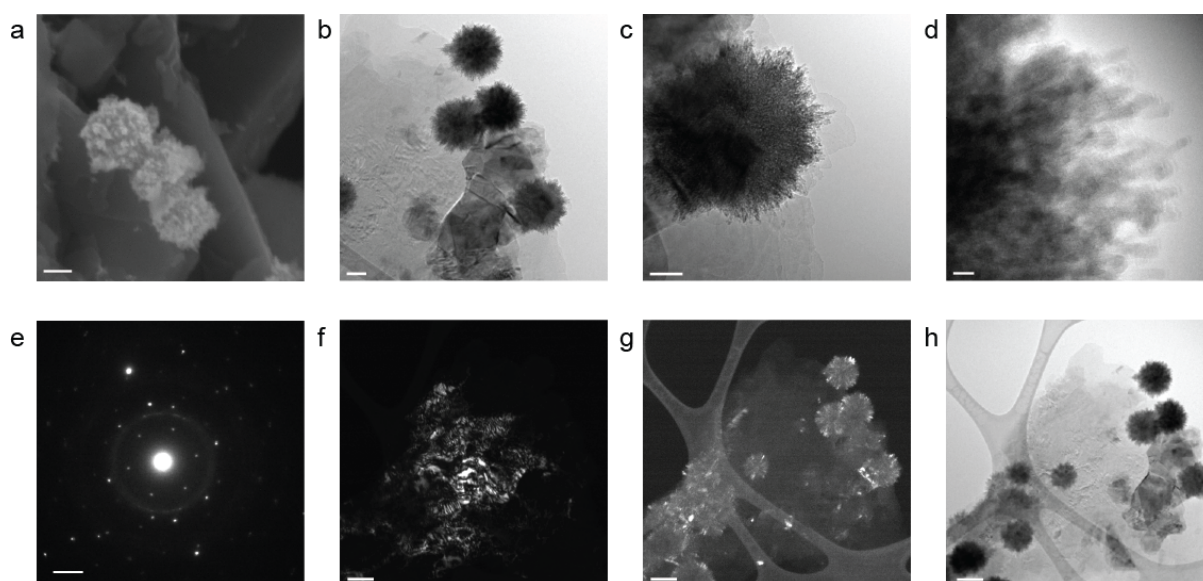

Figure S4. Characterisation of hydrothermal reaction precipitates using sediment MoS$_2$: (a) SEM, scale bar 100 nm. (b) TEM, scale bar 100 nm. (c) TEM, scale bar 50 nm. (d) TEM, scale bar 5 nm. (e) SAED of area shown in (h), scale bar 2 nm^{-1}. (f) Dark field image from spot in (e) showing distribution of MoS$_2$, scale bar 200 nm. (g) Dark field image from ring in (e) showing distribution of ZnS, scale bar 200 nm. (h) TEM, scale bar 200 nm.
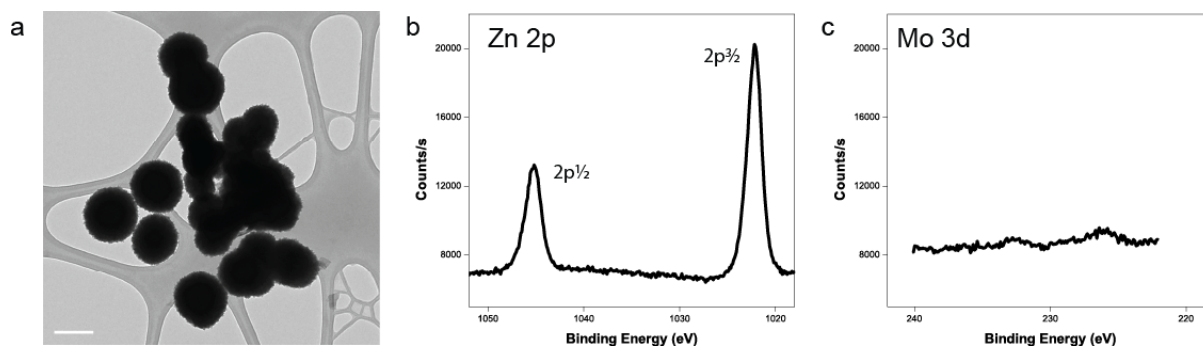
Figure S5. Characterisation of hydrothermal reaction precipitates: (a) TEM image showing spheres of 200-300 nm diameter, scale bar 200 nm. (b) XPS trace of Zn 2p energy range. (c) XPS trace of Mo 3d energy range showing absence of Mo.
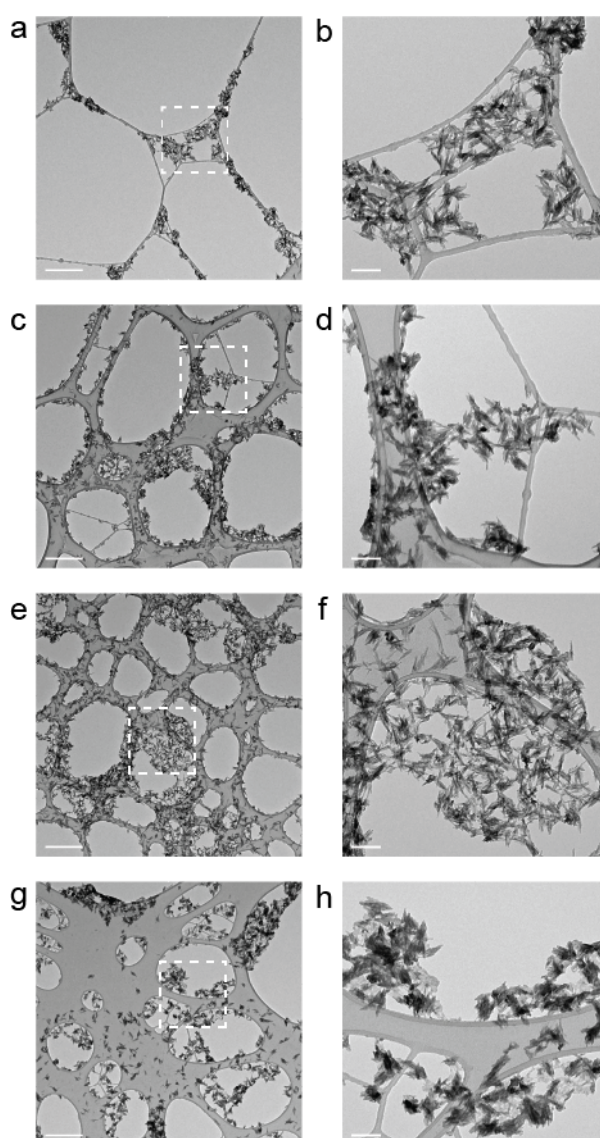

Figure S6. TEM characterisation of hydrothermal reaction supernatants: (a, c, e and g) 0.4, 0.6, 0.8 and 1.0 mM samples, scale bars 500 nm. (b, d, f and h) Higher magnification of the outlined square regions in (a, c, e and g), scale bars 100 nm.
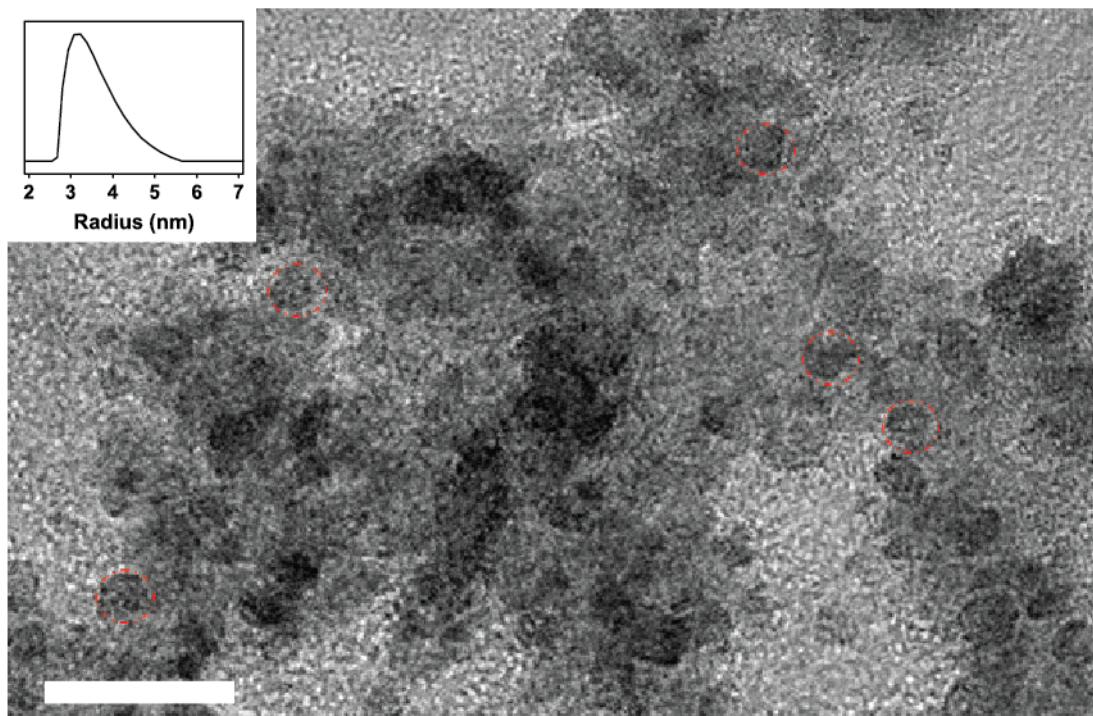
Figure S7. HRTEM of 1 mM sample with outlines of some single particles, scale bar 20nm. Inset number weighted radius statistics from dynamic light scattering of 1 mM sample.
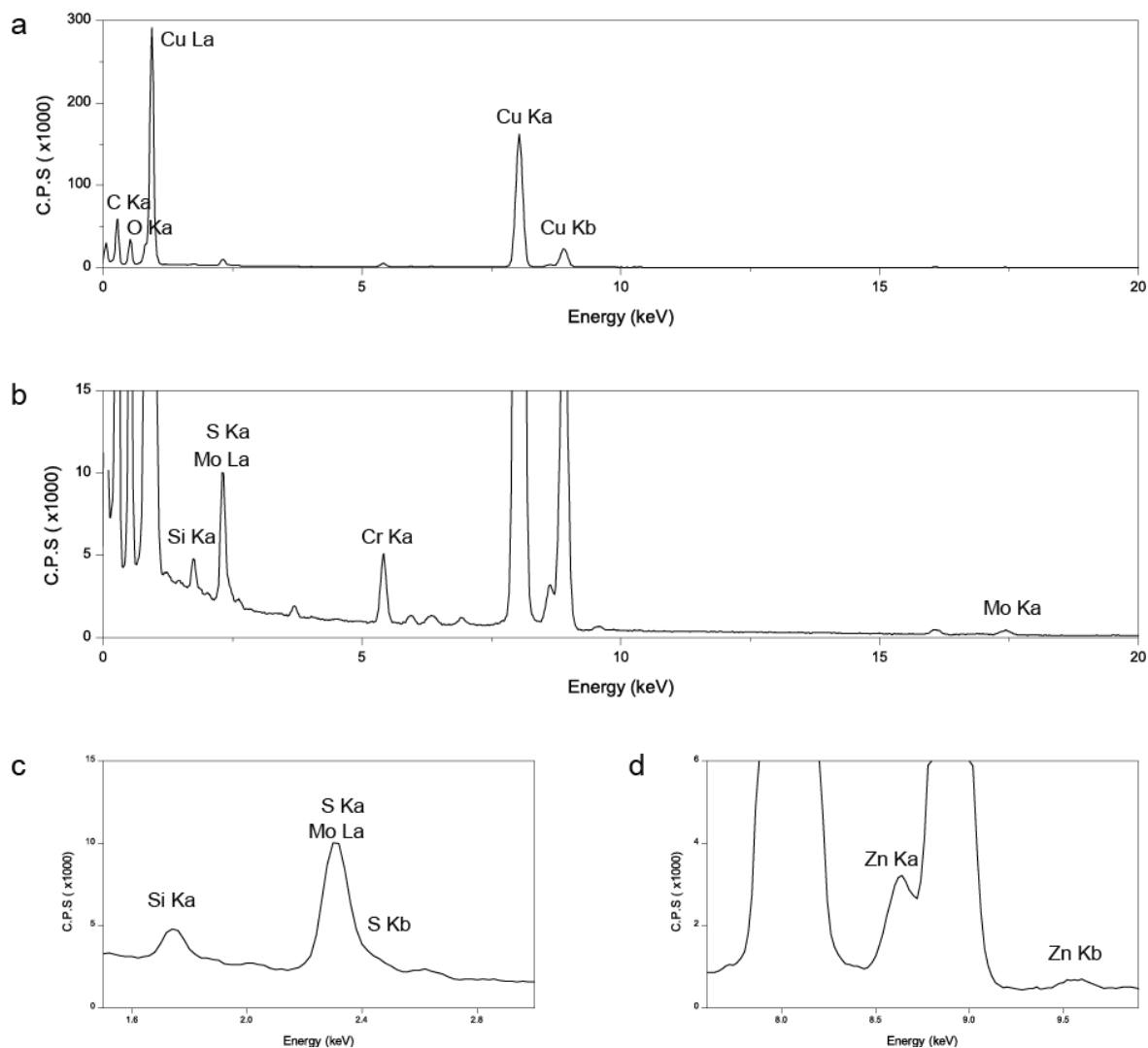
Figure S8. EDX analysis of 0.4 mM hydrothermal reaction supernatant: (a) Full analysis energy range. (b) Magnified baseline showing elemental composition. (c) Region showing overlap of the Mo La and S Ka peaks. (d) Region showing Zn peaks close to the intense Cu peaks from the grid.
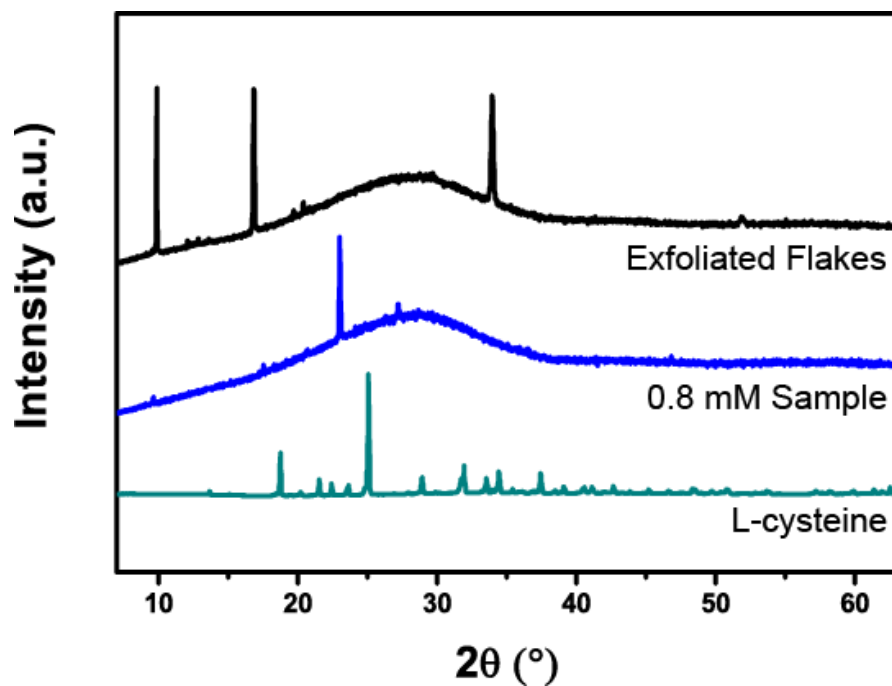
Figure S9. XRD patterns of exfoliated MoS$_2$ flakes (black), 0.8 mM sample (blue) and L-cysteine (green), peaks have been normalized by maximum intensity and offset for ease of comparison. The broad feature centred at approximately 28° in the top two patterns is due to the glass substrates. The 0.8 mM sample has consistent peaks at 9.6 and 17.5° from exfoliated MoS$_2$, and additional peaks at 27.2 and 46.8° from ZnS.[1] After consideration of possible sources, it was found that the prominent peak at 23.0° may be due to unreacted L-cysteine present in the sample.
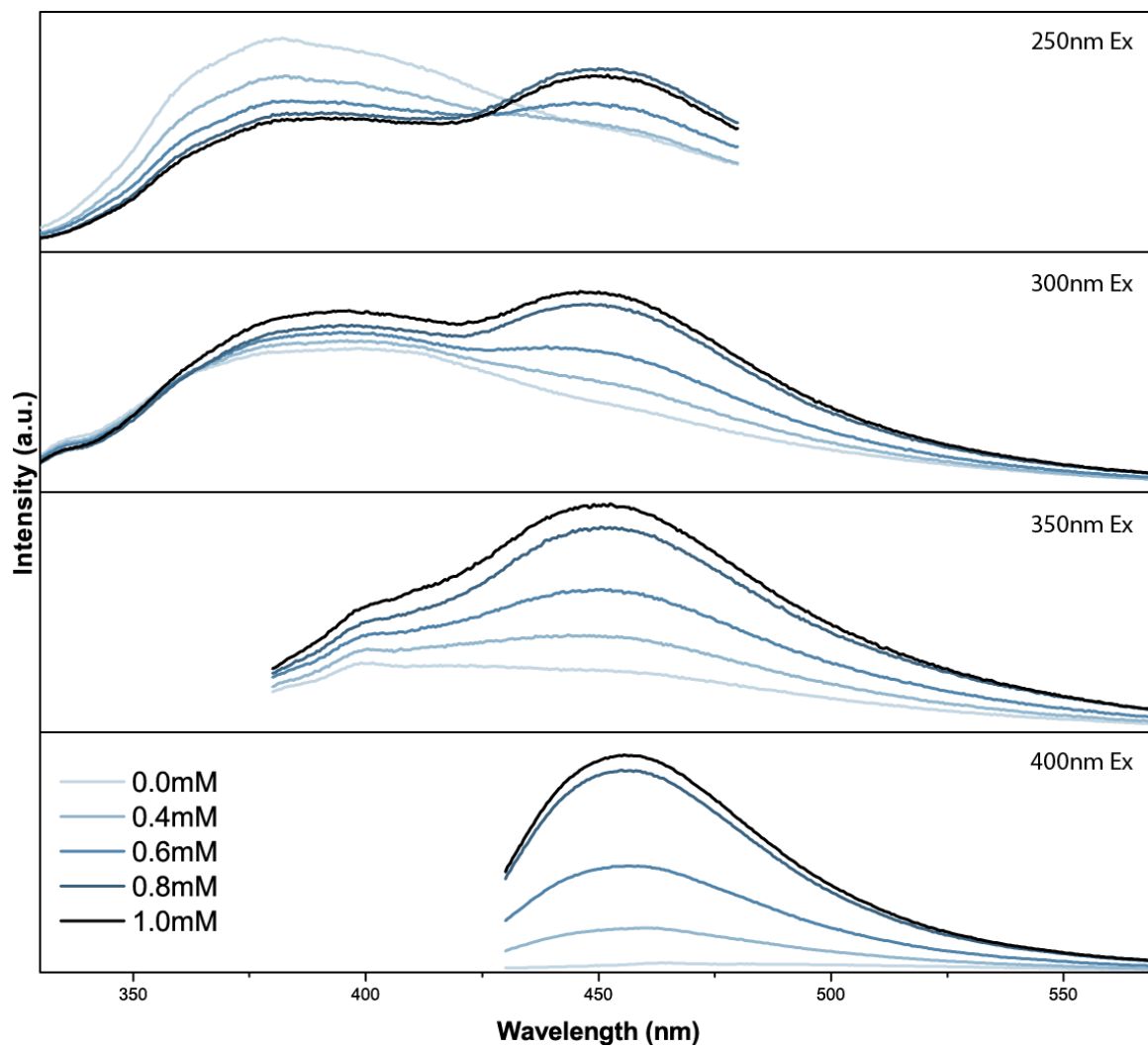
Figure S10. PL emission from hydrothermal reaction supernatants at excitation wavelengths of 250, 300, 350 and 400 nm from 0.0, 0.4, 0.6, 0.8 and 1.0 mM samples.
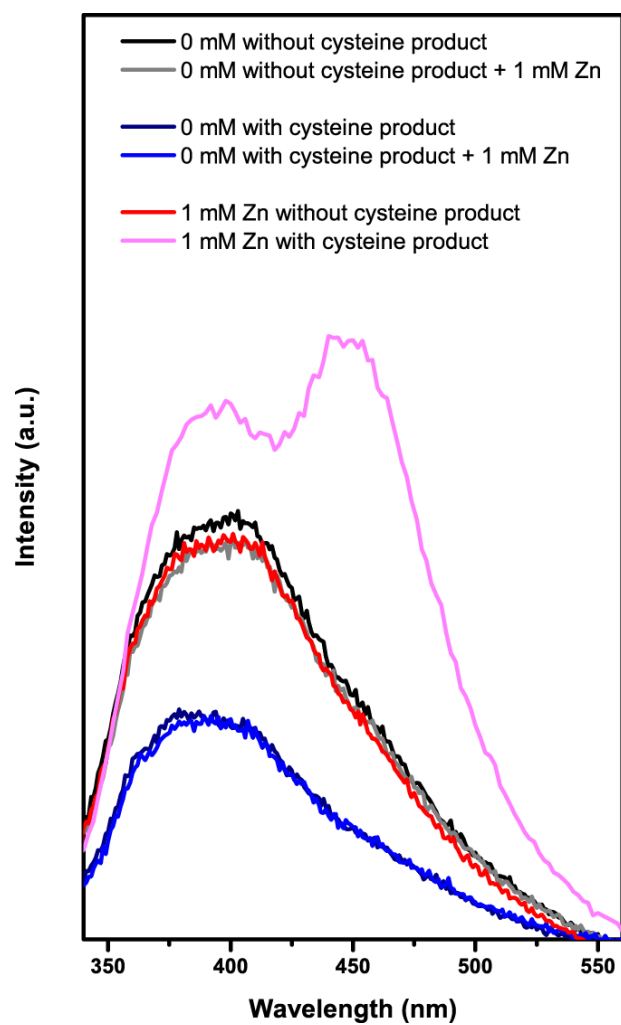
Figure S11. PL emission from products, before and after mixing with zinc nitrate hexahydrate.
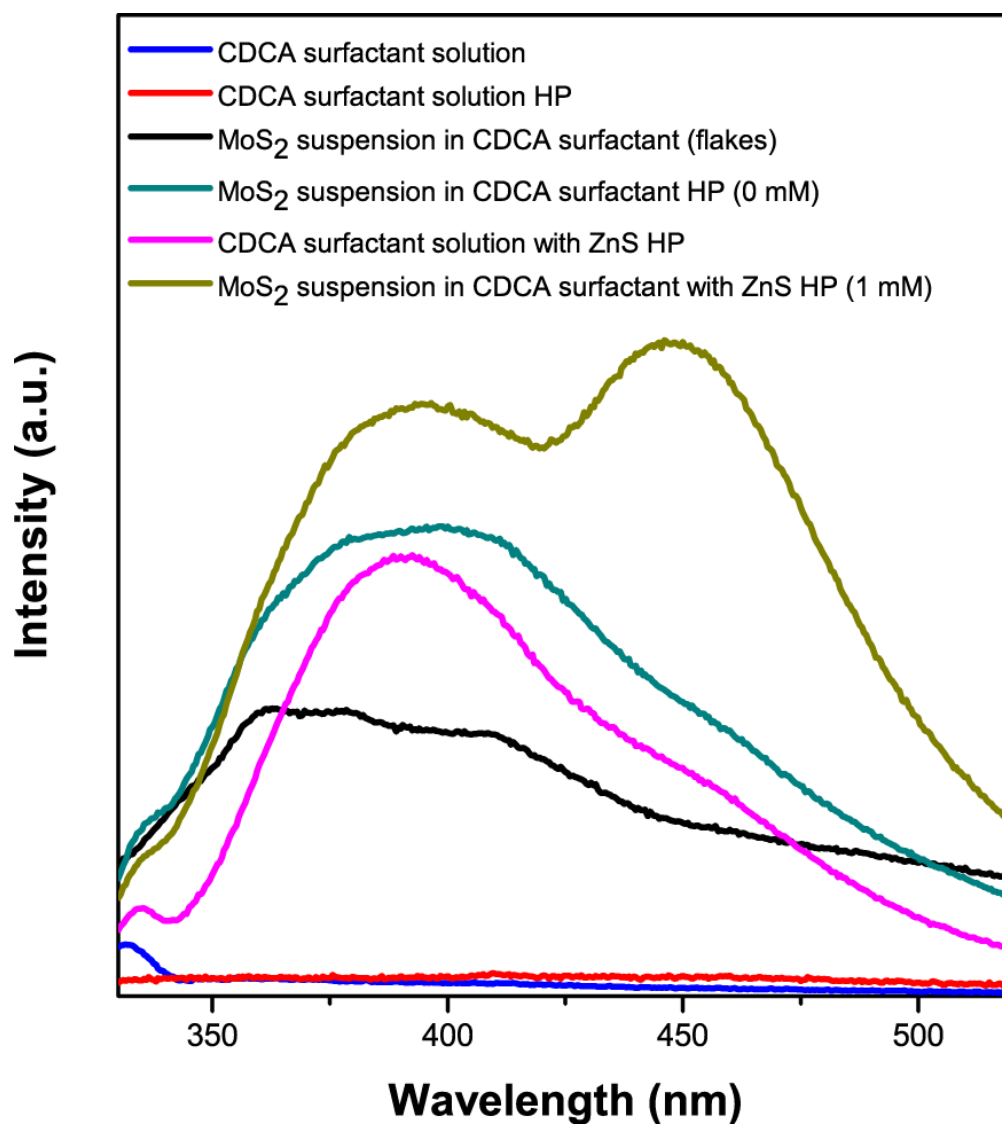
Figure S12. PL emission from surfactant solution and product suspensions, where HP stands for hydrothermal processing.

Table S1. Quantum yield estimations

Sample	Solvent	Refractive Index	Absorbance at 320 nm	Integrated emission	Quantum Yield
Quinine sulphate	0.1 M H_2SO_4	1.33	0.0937	51806.6	54%[2]
0.8 mM sample	MilliQ	1.33	0.0905	1815.6	1.96%

References

1.   G. Wang, B. Huang, Z. Li, Z. Lou, Z. Wang, Y. Dai and M.-H. Whangbo, *Sci. Rep.*, 2015, **5**, 8544.
2.   W. H. Melhuish, *J. Phys. Chem.*, 1961, **65**, 229-235.